NUMERICAL ANALYSIS OF STEEL FIBER-REINFORCED CONCRETE BEAMS FROM TECHNIQUES OF TOPOLOGY OPTIMIZATION

Matheus Barbosa Moreira Cedrim[1], Eduardo Nobre Lages[2],
Aline da Silva Ramos Barboza[2]
[1]Professor, Centro Universitário CESMAC, Maceió, Brazil
matheuscedrim@hotmail.com
[2]Professor, Universidade Federal de Alagoas, Maceió, Brazil
enl@ctec.ufal.br
aline@lccv.ufal.br

ABSTRACT

This work contributes to the fundamentals of structural design aided by topology optimization techniques. Numerical analysis was conducted using the finite element method in ABAQUS® software, employing homogenization models for steel fiber-reinforced concrete (SFRC) in conjunction with the SIMP method. Examples are validated for beam analysis. The results show the influence of optimization procedure parameters, mix proportions, and design requirements. To establish a methodology of analysis that allows for the use of lighter and stronger elements without the traditional incorporation of steel bars into concrete, the case study revealed that, for conventional concretes, reinforcements are necessary to ensure ductile failure.

KEYWORDS: *Steel fiber-reinforced concrete, SIMP, ABAQUS®, Drucker-Prager.*

I. INTRODUCTION

The Brazilian standard NBR 16935 [1] describes fiber-reinforced concrete (FRC) as a composite material characterized by a cementitious matrix with stable discontinuous fibers in an alkaline environment. Among the possibilities for developing projects involving fiber-reinforced concrete structures, determining the fiber content and the mechanical response of the composite can be considered complex and requires thorough experimentation and validation.

With recent advances in the building industry, fiber-reinforced cementitious materials have gained prominence in various research domains. Structural modeling and analysis using numerical methods, such as the Finite Element Method (FEM), are subjects of study for many researchers.

Topology optimization is a robust computational tool aiding designers in determining efficient structural configurations. Stoiber and Kromoser [2] note that extensive research has focused on topology optimization using isotropic material with linear elastic behavior. However, there is a lack of studies comparing linear and nonlinear material behaviors, highlighting a research gap in result analysis and structural application fields. For example, concrete in a post-cracking stage often exhibits inherently nonlinear behavior, which should be reflected in numerical models for computational simulation.

In recent years, optimization techniques employing concepts of physical nonlinearity, as well as consideration of multiple loading cases, have been observed in the literature (Schwarz *et al.* [3]; Jung and Gea [4]; Lotfi [5]; Xia *et al*. [6]; Zhao [7]). The recent development enables greater possibilities for simulating static and dynamic behaviors, allowing for the incorporation of different constitutive models for various optimization problems, with objective functions and constraints defined according to the proposed simulation. Although previous studies have explored the Drucker-Prager model in topology optimization procedures [8-9], this paper also focuses on obtaining realistic strength parameters for design applications.

With the progress in 3D printing techniques and additive manufacturing processes, Da [10] comments that it has become possible to manufacture materials designed from a numerical file directly, enabling the opening of routines for new projects. It is not an exaggeration to emphasize that additive manufacturing and topology optimization are a great combination. In the field of research, there is still a need for a systematic and comprehensive study of structural design aided by topology optimization for engineering applications.

In recent decades, global CO_2 emissions have been increasing significantly. The cement industry plays a relevant role in reducing these gases. To implement more efficient strategies, advances in materials technology and manufacturing processes are alternatives for sustainability. Pressmair *et al.* [11] comment that there are several strategies to reduce the use of cement in concrete structures while preserving performance. Structural optimization as a mathematical tool can provide lighter and higher-strength structural designs.

In this context, concrete structures can benefit from the rational use of raw materials, meeting regulatory requirements, and promoting sustainable development. Conventional structures can be replaced with more economical and durable geometries through 3D printing. In this context, fiber-reinforced concrete has emerged as an attractive alternative for various projects. This work proposes developing a numerical analysis methodology to assist in the design of structural elements made of steel fiber-reinforced concrete (SFRC). This systematic approach involves verifying the load-carrying capacity using the model obtained through topology optimization. It incorporates the homogenized linear elastic behavior and the elastoplastic behavior of SFRC based on the Drucker-Prager model.

The structure of this article is organized as follows: first, a theoretical reference provides a comprehensive review of the fundamental concepts underlying the study; this is followed by the results obtained in the numerical analysis and a discussion of the main contributions of the research.

II. THEORETICAL REFERENCE

This section provides a theoretical framework for steel fiber-reinforced concrete, encompassing topics such as homogenization methods, constitutive models and the assessment of material mechanical properties. It also describes topology optimization techniques for nonlinear materials.

2.1. Steel fiber-reinforced concrete (SFRC) properties

The addition of discontinuous and randomly distributed fibers in the matrix acts as structural reinforcement, allowing for control over crack initiation and propagation in the concrete element. As a result, there is a modification in the mechanical behavior after the rupture (cracking) of the matrix, enhancing the concrete's energy absorption capacity and reducing material brittleness [1].

Mehta and Monteiro [12] categorize SFRC according to the volume fraction of fibers in the mix. It can be classified into three categories: mixes with a low volume fraction (less than 1%), which reduce shrinkage cracking and are commonly used in slabs and pavements with extensive exposed surfaces. Mixes with a moderate volume fraction (between 1% and 2%) increase fracture toughness and impact resistance and are generally used in shotcrete. Lastly, mixes with a high volume fraction (greater than 2%) induce strain-hardening in the composite, resulting in high-performance materials.

Singh [13] illustrates that longitudinal reinforcements behave differently in conventional structural elements depending on the percentage of available steel in the section. In contrast, for SFRC elements, failure occurs once the deformation in the tensioned face reaches a critical value. Typically, the design value for crack width defines the critical value for allowable tensile deformation in this type of structure. Key fiber parameters, including aspect ratio, anchorage, and volume fraction, are specified for post-cracking reinforcement of the concrete.

The analysis of heterogeneous materials using numerical methods requires the description of physical properties that characterize mechanical behavior. For instance, in the linear elastic range, parameters like longitudinal modulus of elasticity and Poisson's ratio are employed considering isotropic behavior. Due to the heterogeneity characteristics, adopting a process aiming at material homogenization is common, thus defining effective properties. Literature often employs homogenization methods for fiber-reinforced concrete elements based on mean fields micromechanics.

The Mori-Tanaka model can be deemed suitable for considering the effective elastic properties of steel fiber-reinforced concrete [14]. Given the identification of two phases, the concrete matrix and the fibers, present in moderate and low quantities, other analytical models, such as the dilute concentration and self-consistent models, yield similar results for fibers with a low volume fraction (typically less than 5%).

Generally, a composite material's strength criterion can be determined by considering the individual strength properties of its phases (matrix and fibers) and their respective volume fractions. The adopted formulation [14] allows for considering any strength criterion for the composite components. Regarding fibers, only their compressive and uniaxial tensile strengths are necessary. The strength of the concrete matrix, in the proposal of the mentioned author, is characterized by the Drucker-Prager criterion.

Dutra *et al.* [15] assessed the strength properties of SFRC based on homogenization and limit analysis. The efficiency of this approach is compared with numerical solutions using the finite element method and subsequently validated against experimental results from the literature. The approximations for predicting the material's resistance behavior are considered satisfactory.

Venkateshwaran *et al.* [16] explain that the mechanical properties of SFRC are influenced by the compressive strength of the cementitious matrix and the fiber reinforcement index (*RI*), which is calculated as the product of the volume fraction and the aspect ratio of the fibers. This study introduces empirical formulas for determining flexural residual stresses [17]. It was found that the obtained strengths are directly proportional to *RI*, the square root of the compressive strength of the matrix, and the square of the number of hooks at the fiber ends. The authors also account for the size effect through a factor related to the fiber length. The characteristic values are detailed in the following equations:

$$f_{L,k} = 0.590 \cdot \sqrt{f_c{}'} + 0.915 \cdot RI \qquad \text{Eq. (1)}$$
$$f_{R1,k} = \psi \cdot [0.226 \cdot \sqrt{f_c{}'} + 5.447 \cdot RI - 0.149 \cdot N^2] \qquad \text{Eq. (2)}$$
$$f_{R2,k} = \psi \cdot [0.250 \cdot \sqrt{f_c{}'} + 6.506 \cdot RI + 0.102 \cdot N^2] \qquad \text{Eq. (3)}$$
$$f_{R3,k} = \psi \cdot [0.201 \cdot \sqrt{f_c{}'} + 6.830 \cdot RI + 0.182 \cdot N^2] \qquad \text{Eq. (4)}$$
$$f_{R4,k} = \psi \cdot [0.177 \cdot \sqrt{f_c{}'} + 6.151 \cdot RI + 0.137 \cdot N^2] \qquad \text{Eq. (5)}$$

where $\psi = \sqrt{1 + L_f/100}$, L_f is the fiber length in millimeters, $f_c{}'$ is the uniaxial compression strength of the matrix and N is the number of hooks.

2.2. Drucker-Prager elastoplastic model

According to Oliveira *et al.* [18], numerous constitutive models utilize a phenomenological approach. They describe the material from a macroscopic perspective, disregarding microscopic mechanisms and considering it continuous and homogeneous.

For the numerical analysis of concrete, it is common to employ failure criteria to verify strength parameters. According to Chen [19], a failure or fracture criterion is described in terms of stress invariants, which may consider the material's yield surface. Much work has been conducted considering the von Mises criterion, the modified von Mises criterion (or Drucker-Prager criterion), and the Coulomb or modified Coulomb criterion.

Considering the Drucker-Prager model [20] as a strength criterion, it can be used for simulating brittle materials such as concrete, soils, and rocks. Souza Neto *et al.* [21] exemplify that in plane stress problems, an approximation that may be valid for concrete wall structures, it could be convenient to use an approach that simultaneously satisfies both the Mohr-Coulomb and Drucker-Prager criteria in uniaxial tension and uniaxial compression states. For the Mohr-Coulomb criterion to be applicable with a given tensile strength f_t' and a given compressive strength f_c', the parameters c and ϕ can be assumed as:

$$\phi = arcsin\left(\frac{f_c' - f_t'}{f_c' + f_t'}\right) \qquad \text{Eq. (6)}$$

$$c = \frac{f_c' \cdot f_t'}{f_c' - f_t'} \cdot \tan\phi \qquad \text{Eq. (7)}$$

where ϕ is the friction angle and c is the cohesion of the material.

Dutra [14] proposed, for steel fiber-reinforced concrete (SFRC), through a homogenization model considering the Drucker-Prager strength criterion for the matrix, the following expressions for the uniaxial compressive strength (f_c^{SFRC}) and biaxial compressive strength (f_{cb}^{SFRC}) of the composite, respectively.

$$\alpha_m = \frac{f_{cbm} - f_{cm}}{2 \cdot f_{cbm} - f_{cm}} \quad \text{Eq. (8)}$$

$$f_c^{SFRC} = \frac{(2+\alpha_m) \cdot \left(\frac{f}{3}\right) \cdot \sigma_f^+ + (1+\alpha_m) \cdot \sigma_m}{(\alpha_m - 1)} \quad \text{Eq. (9)}$$

$$f_{cb}^{SFRC} = \frac{(2-\alpha_m) \cdot \left(\frac{f}{3}\right) \cdot \sigma_f^+ + (1+\alpha_m) \cdot \sigma_m}{(2\alpha_m - 1)} \quad \text{Eq. (10)}$$

where α_m and σ_m are the Drucker-Prager parameters calculated for the matrix, f is the volume fraction of fibers and σ_f^+ is the fiber uniaxial tensile strength.

Dutra [14] notes that for volume fractions under 5%, the aspect ratio of the fibers has a minimal impact on determining the composite's uniaxial compressive and tensile strengths. Consequently, in this model, the studies are limited to fiber percentages below the proposed threshold. Therefore, the determining factors are defined as the volume fraction of the fibers and their mechanical characteristics, in addition to the mechanical characteristics of the cementitious matrix without the addition of fibers.

It is considered that most of the data available in the literature for SFRC under biaxial loading, based on experimental evaluations, show little or no results regarding the material under tensile stresses. Therefore, it is assumed that the tensile strength for SFRC (f_t^{SFRC}) and for plain concrete is the same as obtained for the composite under uniaxial loading. Hence, the relationship proposed by the fib Model Code 2010 [22] was used.

$$f_t^{SFRC} = 0.3 \cdot (f_c^{SFRC})^{2/3} \quad \text{Eq. (11)}$$

Aligned with the works of Dutra [14] and Matos [23], the consideration of a homogeneous continuous medium is employed. Initially, the assumption is made that fibers are randomly distributed within the concrete matrix, both treated as homogeneous. Subsequently, the Representative Volume Element (RVE) of the heterogeneous medium is defined, aiming to establish the material's strength. With these properties of the homogeneous medium defined, in the final stage, it becomes possible to assess the mechanical properties of the structure.

2.3. Nonlinear materials topology optimization

Among the topology optimization approaches, Wang *et al.* [24] highlight: density-based methods, level-set method, methods based on differential equations, and methods based on geometric components.

The most well-known material model for finite element-based topology optimization is the Solid Isotropic Material with Penalization (SIMP) model, developed in the 1980s by Bendsøe and Kikuchi [25]. The SIMP acronym stands for Solid Isotropic Material with Penalization. Sometimes, the model is referred to as material interpolation, artificial material, power law, or density method, but SIMP is the most recognized terminology globally [26].

With the advancing applications of topology optimization techniques, there is a wide array of educational codes and commercial software based on the SIMP model, as presented in the work by Wang *et al.* [24].

Despite considering a homogeneous and isotropic material in its formulation, SIMP, as explained by Wu *et al.* [27], can be interpreted as a multiscale approximation (Figure 1) [28]. Based on this, a heterogeneous material distribution within the element domain can be used to determine material properties for an intermediate density.

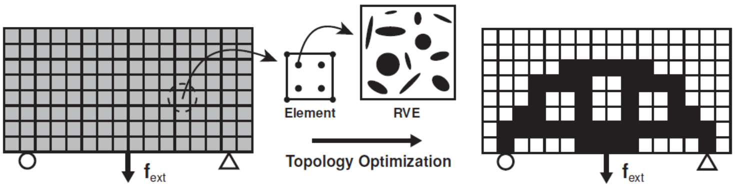

Figure 1. Example of multiscale structures topology optimization

In the discrete formulation of the problem, minimizing the strain energy (c), we have:

$$\min c(\mathbf{x}) = \boldsymbol{U}^T \boldsymbol{K} \boldsymbol{U} = \sum_{e=1}^{N} (x_e)^p \boldsymbol{u}_e^T \boldsymbol{k}_e \boldsymbol{u}_e$$
$$\text{s.t. } V(\boldsymbol{x}) = vf\ V_0 \qquad \text{Eq. (12)}$$
$$0 < x_{min} \le x_e \le 1$$

where $\boldsymbol{U}$ and $\boldsymbol{F}$ are the global displacement and force vectors, respectively, $\boldsymbol{K}$ is the global stiffness matrix, $\boldsymbol{u_e}$ and $\boldsymbol{k_e}$ are the element displacement vector and stiffness matrix, respectively, $\boldsymbol{x}$ is the vector of design variables (relative densities of elements), $\boldsymbol{x_{min}}$ is a vector of minimum relative densities, N is the number of elements used to discretize the design domain, p is the penalty factor, $V(\boldsymbol{x})$ and V_0 are the material volume and design domain volume, respectively, and vf is the prescribed volume fraction.

Gaganelis *et al.* [29] introduce the concept of Optimization-Aided Design (OAD), a methodology focused on optimizing the design and sizing of structures through advanced optimization techniques. This approach encompasses discovering the optimal shape, identifying reinforcement layouts, and utilizing appropriate cross-sectional profiles for reinforced concrete.

The OAD framework offers a versatile methodology that can be applied to different application areas. This approach can be employed for any type of concrete (ranging from normal to ultra-high strength), along with arbitrary types of reinforcement (steel, carbon, fibers). Furthermore, it can be extended to various fields of structural engineering, such as steel structures, wood, and foundations.

Wen *et al.* [30] review the application of topology optimization methods for nonlinear problems. In engineering practice, several issues may be considered nonlinear; however, it is common to treat them as linear for simplification. This simplification can lead to significant errors and even incorrect results, posing risks to structural integrity. From a computational perspective, introducing nonlinearity poses challenges in solving the study equations due to local and global instability and excessive distortion of low-density elements.

Schwarz *et al.* [3] note that an incremental process is required in problems involving material nonlinearity, where the material response depends on the applied load intensity. Consequently, the sensitivities involved in the optimization process must be calculated after each incremental step. Like state variables, derivatives are updated through increments added to the previous steps.

Lotfi [5] emphasizes that other numerical instabilities may arise due to nonlinearity in structural problems. For instance, some instabilities may be associated with modeling elements with low density and excessive distortion of elements. The computational cost should also be underscored, as the nonlinear iterative finite element analysis typically accounts for approximately 90% of the effort in solving an optimization problem.

Simulia [31] demonstrates the solution process through Newton's method for nonlinear analysis. In a mechanical problem, the sum of forces at a point must be zero for static equilibrium. For each iteration in nonlinear analyses, the default processor of ABAQUS/CAE® assembles the stiffness matrix of the model and solves the system of equations. The computational cost of each iteration is close to the cost of a complete linear analysis, making the computational demand of a nonlinear analysis potentially higher than that of a linear analysis.

Thus, the flowchart presented in Figure 2 illustrates the steps to solve the problem proposed in this work.

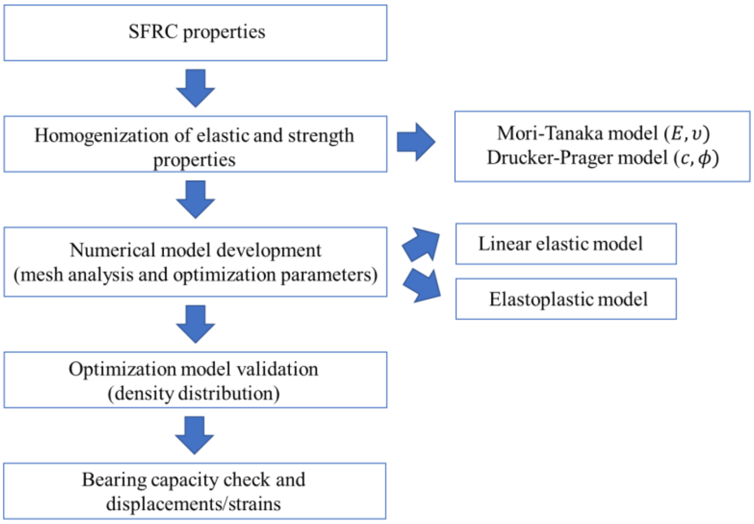

Figure 2. Flowchart of the optimized design routine

III. RESULTS AND DISCUSSIONS

For the computational simulation of the examples in this work, the software ABAQUS® 2019 is used for integrated finite element analysis and optimization processes. The results are obtained using a notebook with an Intel Core i7-12700H processor, 16 GB of RAM, and the Windows 11 Home 64-bit operating system.

The load application region is not considered in the optimization process. The density update strategy is normal. The solution algorithm is general. The sensitivity filter is automatically defined according to the mesh's characteristic dimension. The material interpolation technique used is SIMP. The other details are listed in Table 1.

The penalty factor (p) is an important parameter to avoid numerical instabilities. Christensen and Klarbring [32] suggest gradually increasing the p-value from 1 to 4, which aids in convergence. However, in this study, the penalty factor is considered constant throughout the entire optimization procedure.

Table 1. Topology optimization parameters

Parameters of the SIMP method	Value
Minimum density (ρ_{min})	0.001
Maximum density (ρ_{max})	1
Maximum change of the density per cycle of the project	0.25
Penalty factor (p)	3
Maximum tolerance for the objective function	0.001
Maximum tolerance for the element density	0.005

3.1. Clamped beam: analysis of strength parameters

For this analysis, a clamped beam with a length of $L = 5.0\ m$ and a cross-sectional width of $20\ cm$ and height of $50\ cm$ was modeled, as shown in Figure 3. The applied load was $60\ kN/m$ uniformly distributed at the top (equivalent to a pressure of $300\ kN/m^2$), and the ends have displacement restrictions in two directions. The characteristic mesh size for the plane stress elements was set to

60 mm. A volume fraction (vf) constraint of 50% was considered when generating all the results presented.

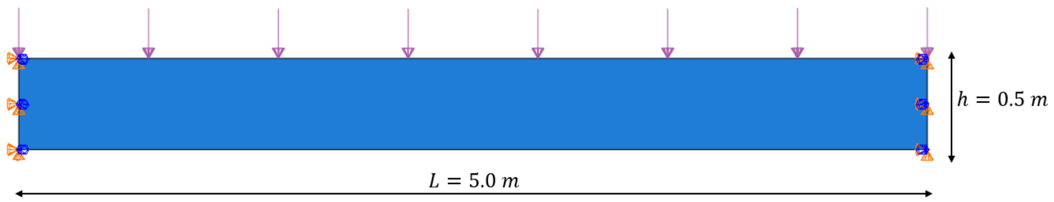

Figure 3. Adopted model in the parametric analysis

To analyze the influence of fiber content in the optimized models, three different fiber contents (0.5%, 1.0%, and 1.5%) were used for five concrete strength classes (30 to 50 MPa) (Tables 2, 3, and 4). For all cases, $f_{cbm} = 1.16 \cdot f_{cm}$ was considered. Tensile strength was determined using the fib Model Code 2010 equation [22].

Table 2. SFRC strength parameters (*f* = 0.5%)

f_{cm} (MPa)	f_c^{SFRC} (MPa)	f_{cb}^{SFRC} (MPa)	f_t^{SFRC} (MPa)	E (MPa)	υ	c (MPa)	ϕ (º)
30	34.02	38.93	3.15	30832.63	0.2	5.18	56.15
35	39.02	44.73	3.45	32994.25	0.2	5.80	56.88
40	44.02	50.53	3.74	34993.57	0.2	6.42	57.50
45	49.02	56.33	4.02	36861.19	0.2	7.02	58.05
50	54.02	62.13	4.29	38619.22	0.2	7.61	58.53

Table 3. SFRC strength parameters (*f* = 1.0%)

f_{cm} (MPa)	f_c^{SFRC} (MPa)	f_{cb}^{SFRC} (MPa)	f_t^{SFRC} (MPa)	E (MPa)	υ	c (MPa)	ϕ (º)
30	38.04	43.06	3.39	31151.14	0.2	5.68	56.74
35	43.04	48.86	3.68	33319.09	0.2	6.30	57.38
40	48.04	54.67	3.96	35323.91	0.2	6.90	57.95
45	53.04	60.47	4.23	37196.35	0.2	7.50	58.44
50	58.04	66.24	4.50	38958.65	0.2	8.08	58.89

Table 4. SFRC strength parameters (*f* = 1.5%)

f_{cm} (MPa)	f_c^{SFRC} (MPa)	f_{cb}^{SFRC} (MPa)	f_t^{SFRC} (MPa)	E (MPa)	υ	c (MPa)	ϕ (º)
30	42.07	47.2	3.63	31471.62	0.2	6.18	57.27
35	47.07	53.0	3.91	33645.91	0.2	6.78	57.84
40	52.07	58.8	4.18	35656.22	0.2	7.38	58.35
45	57.07	64.6	4.47	37533.47	0.2	7.96	58.81
50	62.07	70.4	4.70	39300.04	0.2	8.54	59.22

Following the post-processing stage where surfaces were extracted, considering density values above $\rho > 0.25$ and using a moderate filtering technique, the structural behavior analysis of optimal topologies was performed (Figures 4 and 5). The original model has a $0.5\ m^3$ volume. The optimized ones vary from 0.351 to $0.374\ m^3$.

With the homogenized material data, a nonlinear analysis was carried out for each surface to construct the load-displacement curves and identify the maximum plastic strains. CPS4 elements with a characteristic mesh size of $60\ mm$ were used. In all cases, the monitored displacement was considered at the bottom in the middle of the span.

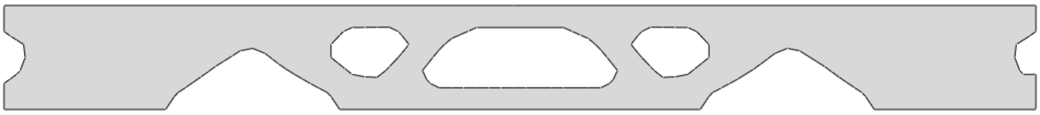

Figure 4. Linear elastic optimized extracted surface

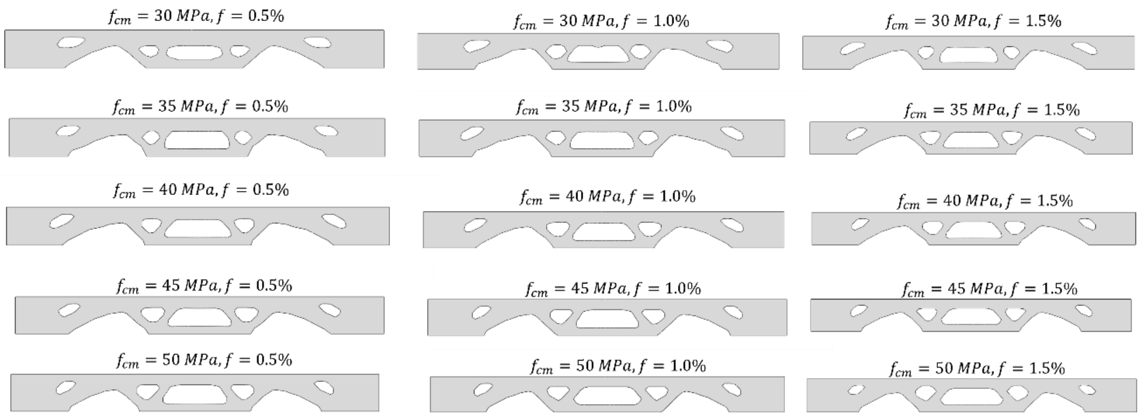

Figure 5. Elastoplastic optimized extracted surfaces

Considering the defined strength parameters, the load-displacement curves in Figures 6, 7 and 8 show that smaller displacements occur as the matrix strength increases along with the fiber content.

In Figure 6, the highest displacement is obtained by the model with $f_{cm} = 30\ MPa$, approximately $5.69\ mm$. In Figure 7, the maximum value is $3.87\ mm$. Finally, in Figure 8, the highest recorded value is $3.31\ mm$.

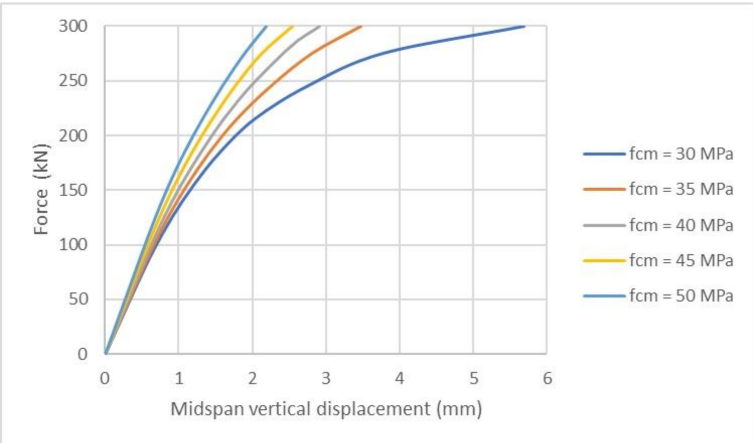

Figure 6. The load-displacement curve for optimized models (*f* = 0.5%)

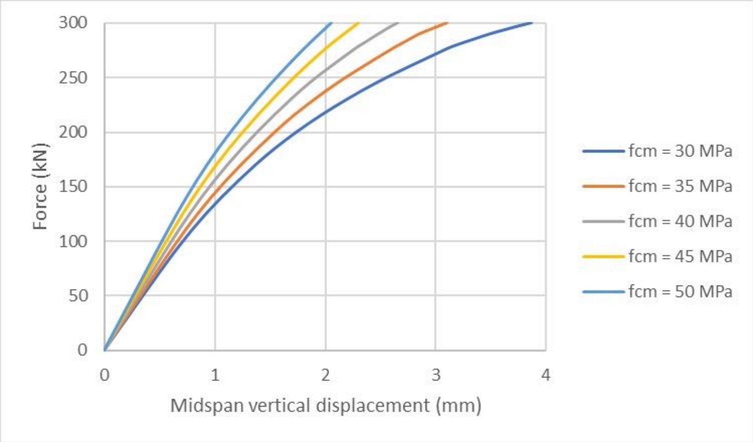

Figure 7. The load-displacement curve for optimized models (*f* = 1.0%)

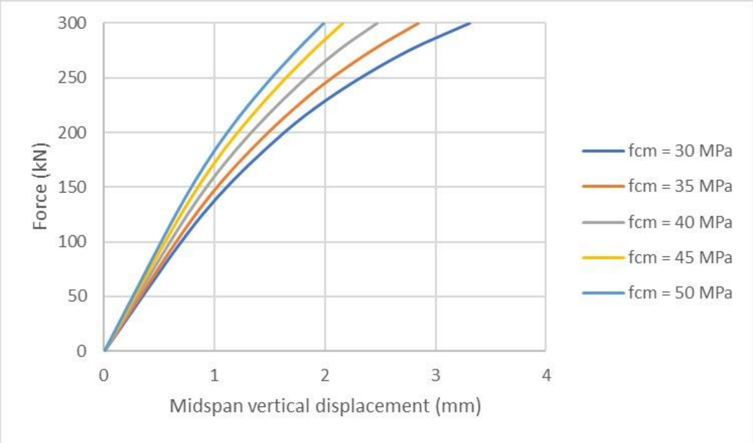

Figure 8. The load-displacement curve for optimized models (*f* = 1.5%)

The equations proposed by [16] were chosen for the empirical prediction of characteristic stresses in bending. In this analysis, a fiber length of $60\,mm$, an aspect ratio ($L/D = 60$), and hooks at the ends ($N = 2$) are considered (Table 5, Table 6, and Table 7).

It is observed that the uniaxial tensile strength of the fibers does not have a predominant effect on the residual strengths. However, longer fibers, maintaining the aspect ratio, tend to develop higher strengths than shorter fibers, indicating the presence of the size effect.

According to [1], the minimum relationships between strengths are met ($\frac{f_{R1k}}{f_{Lk}} \geq 0.40$ and $\frac{f_{R3k}}{f_{R1k}} \geq 0.50$), allowing for the total or partial substitution of conventional reinforcement in structural elements designed in the Ultimate Limit State (ULS).

Table 5. SFRC properties (*f* = 0.5%)

f_{cm} (MPa)	f_{lk} (MPa)	f_{r1k} (MPa)	f_{r2k} (MPa)	f_{r3k} (MPa)	f_{r4k} (MPa)	f_{r1k}/f_{lk} (MPa)	f_{r3k}/f_{r1k} (MPa)	Class
30	3.51	2.88	4.72	4.91	4.25	0.82	1.70	2e
35	3.76	3.00	4.86	5.02	4.35	0.80	1.67	3e
40	4.01	3.12	4.98	5.12	4.44	0.78	1.64	3e
45	4.23	3.23	5.11	5.22	4.53	0.76	1.62	3e
50	4.45	3.33	5.22	5.31	4.61	0.75	1.59	3e

Table 6. SFRC properties (*f* = 1.0%)

f_{cm} (MPa)	f_{lk} (MPa)	f_{r1k} (MPa)	f_{r2k} (MPa)	f_{r3k} (MPa)	f_{r4k} (MPa)	f_{r1k}/f_{lk} (MPa)	f_{r3k}/f_{r1k} (MPa)	Class
30	3.78	4.95	7.19	7.50	6.59	1.31	1.52	4e
35	4.04	5.07	7.32	7.61	6.69	1.26	1.50	5e
40	4.28	5.19	7.45	7.71	6.78	1.21	1.49	5e
45	4.51	5.30	7.58	7.81	6.86	1.18	1.47	5e
50	4.72	5.40	7.69	7.90	6.94	1.14	1.46	5e

Table 7. SFRC properties (*f* = 1.5%)

f_{cm} (MPa)	f_{lk} (MPa)	f_{r1k} (MPa)	f_{r2k} (MPa)	f_{r3k} (MPa)	f_{r4k} (MPa)	f_{r1k}/f_{lk} (MPa)	f_{r3k}/f_{r1k} (MPa)	Class
30	4.06	7.01	9.65	10.09	8.92	1.73	1.44	7e
35	4.31	7.14	9.79	10.20	9.02	1.65	1.43	7e
40	4.55	7.26	9.92	10.30	9.11	1.59	1.42	7e
45	4.78	7.36	10.04	10.40	9.20	1.54	1.41	7e
50	5.00	7.47	10.16	10.49	9.28	1.50	1.41	7e

Verifications at the ULS are conducted by analyzing load-bearing capacity following the topology optimization process. In the presented examples, where geometric discontinuities exist in the resulting topologies, the most appropriate procedure for structural safety analysis involves using strut-and-tie models, where the struts represent compressed concrete, and the ties represent the contribution of fibers and steel bars in the section.

In a simplified approach, to determine the internal forces (Figure 9), the model is treated as a linear solid element of a clamped beam without considering the presence of voids. The parameters for SFRC, listed in the previous tables, are applied for different fiber contents.

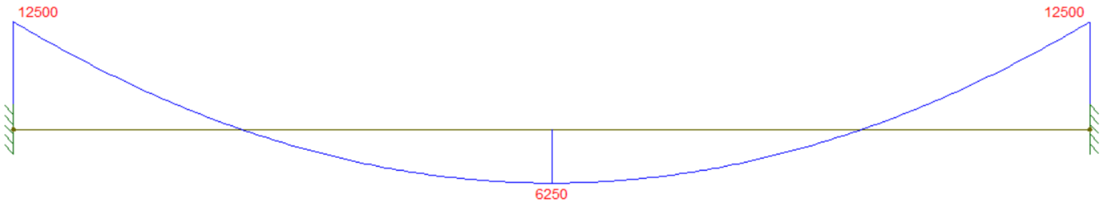

Figure 9. Bending moment characteristic diagram ($kN \cdot cm$)

The rigid-plastic model [1] was used to verify the resistant forces due to bending moments. The resistant behavior (Mu) [1] was investigated with $As = 0$, which led to the condition of rupture of the elements, regardless of the analyzed concrete class (Figure 10). Consequently, despite the norm allowing total or partial replacement of conventional reinforcement, it is observed that the absence of this reinforcement will lead to flexural failure.

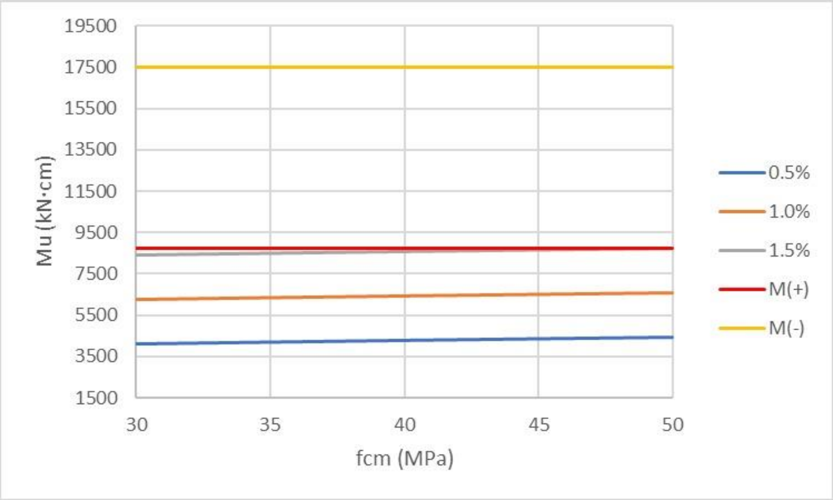

Figure 10. Resistant bending moments for $As = 0$

Considering the absence of transverse reinforcement in the member, the design tensile strength is calculated for the applied shear force $V_{Sd} = 210\ kN$ (Figure 11). As the maximum principal stresses in the optimized models are on the order of 0.5 kN/cm^2 (Figure 12), it eliminates the possibility of ensuring shear strength without longitudinal reinforcements.

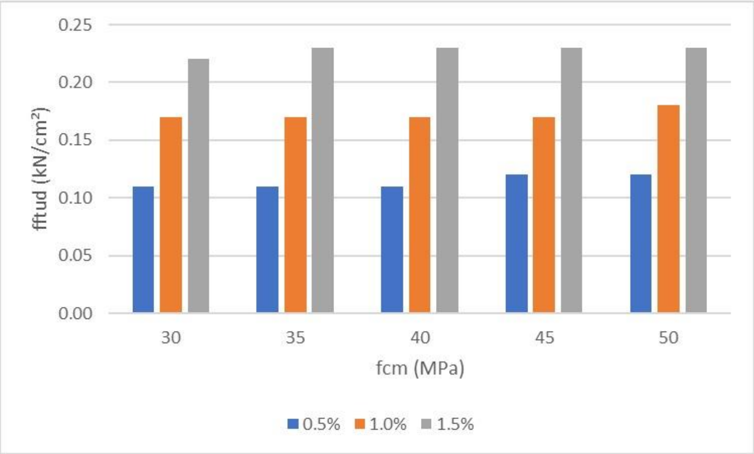

Figure 11. Design tensile strength of SFRC (f_{ftud})

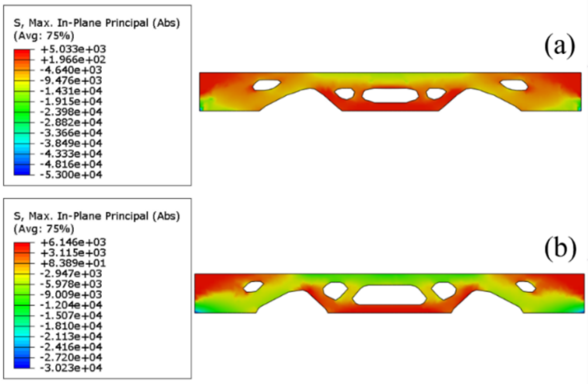

Figure 12. Maximum principal stresses in kPa
(a) $f_{cm} = 30\ MPa\ and\ f = 0.5\%$ (b) $f_{cm} = 50\ MPa\ and\ f = 1.5\%$

It is concluded that longitudinal and transverse reinforcements are necessary for this structural element configuration to achieve shear capacity. The use of fibers contributes to the overall behavior of the element; however, it is insufficient to prevent shear failure.

In the context of conventional concretes, elements with $f_{cm} \leq 50\ MPa$ were analyzed, which became a limitation for the investigated applications. Due to the adopted strength model, the fiber content was also limited to 5%. In the practice of common constructions, this content can be considered up to 1%. However, as described by the equations and models, fibers enhance the post-cracking behavior and provide a strength gain for typical reinforced concrete elements.

Although topology optimization is a tool in the decision-making process for steel fiber-reinforced concrete design, it is essential to complement it with normative checks to ensure that the numerical models accurately reflect real-world conditions. As observed, despite ensuring ductility, project validation is necessary.

IV. CONCLUSIONS

Several parameters, including the microstructure of the concrete matrix, fiber content, fiber shape and geometry, fiber distribution, and matrix-fiber interface, can significantly influence SFRC's behavior. This variability justifies the diverse structural responses exhibited by this material.

In addition to the challenge of material characterization, a review was conducted on topology optimization methods, especially for concrete structures. Initially used as a conceptual method, it was noted that over the years, research has intensified to combine mathematical principles with design practices. This leads to maximizing structural efficiency and a better understanding of mechanical behavior in various engineering areas.

Together with the optimization variables (mesh size, filter radius, convergence criteria, etc.) defined by the SIMP method, it was observed that the dosage of SFRC influences the definition of material strength parameters, leading to changes in the found topology. Each case is unique and requires a precise definition for subsequent analyses. Unlike many purely numerical examples found in the literature, combining design aspects for a specific material is an innovative aspect of this work.

In the numerical approach used, homogenized material data were employed with the support of empirical equations for predicting strength. However, laboratory tests should be adopted for a more realistic characterization of the problem and to avoid large statistical variations in understanding the numerical model. The goal was to classify different materials (e.g., classes 3e, 5e, 7e) by normative references, establishing a causality relationship between strength evolution and behavior under loading conditions.

For typical building applications where the height/span ratio is around $1/10$, relying solely on fibers has not proven feasible for the complete replacement of conventional reinforcements. This is justified because Steel Fiber-Reinforced Concrete (SFRC) is more commonly used in practical applications in other segments, such as industrial flooring, concrete designed for tunnel linings and precast elements.

ACKNOWLEDGEMENTS

The authors acknowledge the Laboratory of Scientific Computing and Visualization (LCCV), at the Center of Technology (CTEC), Federal University of Alagoas (UFAL), for its support of this research. The second author acknowledges the support of the Brazilian National Council for Scientific and Technological Development (CNPq) in the development of this work.

REFERENCES

[1]. Brazilian Association of Technical Standards (2021) NBR 16935: Projeto de estruturas de concreto reforçado com fibras – Procedimento. ABNT (in Portuguese)

[2]. Stoiber N., Kromoser B. (2021) Topology optimization in concrete construction: a systematic review on numerical and experimental investigations. Struct. Multidiscipl. Optim. 64(4):1725-1749.

[3]. Schwarz S., Maute K., Ramm E. (2001) Topology and shape optimization for elastoplastic structural response. Comput. Methods Appl. Mech. Eng. 190(15-17):2135-2155.

[4]. Jung D., Gea H. (2004) Topology optimization of nonlinear structures. Finite Elem. Anal. Des. 40(11):1417-1427.

[5]. Lotfi R. (2013) Topology optimization under nonlinear mechanics. Ph.D. dissertation, John Hopkins University.

[6]. Xia L., Fritzen F., Breitkopf P. (2017) Evolutionary topology optimization of elastoplastic structures. Struct. Multidiscipl. Optim. 55:569-581.

[7]. Zhao T. (2021) Nonlinear topology optimization: theory and applications. Ph.D. dissertation, Georgia Institute of Technology.

[8]. Bogomolny M., Amir, O. (2012) Conceptual design of reinforced concrete structures using topology optimization with elastoplastic material modeling. Int. J. Numer. Methods Eng. 90(13):1578-1597.

[9]. Luo Y., Kang Z. (2012). Topology optimization of continuum structures with Drucker–Prager yield stress constraints. Comput. Struct. 90:65-75.

[10]. Da D. (2019) Topology Optimization Design of Heterogeneous Materials and Structures. Wiley.

[11]. Pressmair N., Xia Y., Wu H., Langelaar M., Hendricks M.A., Majdouba A., Mogra M., Grisaro H., Amir O., Kromoser B. (2023) Bridging the gap between mathematical optimization and structural engineering: Design, experiments and numerical simulation of optimized concrete girders. Struct. Conc. 4:5314-5330.

[12]. Mehta P.K., Monteiro P.J.M. (2014) Concreto: microestrutura, propriedades e materiais. Ed. IBRACON. (in Portuguese)

[13]. Singh H. (2017) Steel Fiber Reinforced Concrete: Behavior, Modelling and Design. Springer.

[14]. Dutra V.F.P. (2012) Um modelo constitutivo para o concreto reforçado com fibras de aço via Teoria da Homogeneização. Ph.D. dissertation. Federal University of Rio Grande do Sul, Porto Alegre. (in Portuguese)

[15]. Dutra V.F.P., Maghous S., Campos Filho A. (2013) A homogenization approach to macroscopic strength criterion of steel fiber reinforced concrete. Cement Concr. Res. 44:34-45.

[16]. Venkateshwaran A., Tan K.H., Li Y. (2018) Residual flexural strengths of steel fiber reinforced concrete with multiple hooked-end fibers. Struct. Concr. 19(2):352-365.

[17]. Brazilian Association of Technical Standards (2021) NBR 16940: Concreto reforçado com fibras – Determinação das resistências à tração na flexão (limite de proporcionalidade e resistências residuais) – Método de ensaio. ABNT (in Portuguese)

[18]. Oliveira D.B., Penna S.S., Pitangueira R.L.S. (2020) Elastoplastic constitutive modeling for concrete: a theoretical and computational approach. Rev. IBRACON Estrut. Mater. 13:171-182.

[19]. Chen W.F. (2007) Plasticity in reinforced concrete. J. Ross Publishing.

[20]. Drucker D.C., Prager W. (1952) Soil mechanics and plastic analysis for limit design. J. Appl. Math. 10(2):157-165.

[21]. Souza Neto E.A., Peric D., Owen D.R.J. (2008) Computational methods for plasticity: theory and applications. John Wiley & Sons.

[22]. International Federation for Structural Concrete (2013) fib Model Code for Concrete Structures 2010. Wiley.

[23]. Matos C.C.D. (2021) Análise numérica de vigas em concreto reforçado com fibras de aço via método dos elementos finitos. M.S. thesis. Federal University of Rio Grande do Sul, Porto Alegre. (in Portuguese)

[24]. Wang C., Zhao Z., Zhou M., Sigmund O., Zhang X.S. (2021) A comprehensive review of educational articles on structural and multidisciplinary optimization. Struct. Multidiscipl. Optim. 64(5):2827-2880.

[25]. Bendsøe M.P., Kikuchi N. (1988) Generating optimal topologies in structural design using a homogenization method. Comput. Methods Appl. Mech. Eng. 71(2):197-224.

[26]. Rozvany G.I.N. (2009) A critical review of established methods of structural topology optimization. Struct. Multidiscipl. Optim. 37(3):217-237.

[27]. Wu J., Sigmund O., Groen J.P. (2021) Topology optimization of multi-scale structures: a review. Struct. Multidiscipl. Optim. 63:1455-1480.

[28]. Xia L. (2016) Multiscale structural topology optimization. Elsevier.

[29]. Gaganelis G., Mark P., Forman P. (2022) Optimization Aided Design: Reinforced Concrete. John Wiley & Sons.

[30]. Wen G., Liu J., Chen Z., Wei P., Long K., Wang H., Rong J., Xie Y. (2022) A survey of nonlinear continuum topology optimization methods. Chin. J. Theor. Appl. Mech. 54(9):1-17.

[31]. Simulia (2014) Abaqus® User's Manual volume 2.

[32]. Christensen P.W., Klarbring A. (2009) An introduction to structural optimization. Springer.

Authors

Matheus Barbosa Moreira Cedrim: He graduated with a Bachelor's degree in Civil Engineering from CESMAC University Center in 2016. He earned a Master of Science in Civil Engineering with a concentration in Structures from the Graduate Program in Civil Engineering (PPGEC) at the Federal University of Alagoas (UFAL) in 2019. He is currently pursuing a Ph.D. in Civil Engineering with a concentration in Structures and Materials from the same institution. His research interests focus on structural mechanics, particularly computational numerical methods applied to structural analysis. His main areas of work include civil construction, geotechnics, and concrete structures.

Eduardo Nobre Lages: He earned a Bachelor's degree in Civil Engineering from the Federal University of Alagoas (UFAL) in 1989, followed by a Master's degree in 1992 and a Ph.D. in 1997, both in Civil Engineering with a concentration in Structures from the Pontifical Catholic University of Rio de Janeiro (PUC-RJ). He is a Full Professor at the Center of Technology (CTEC) at the Federal University of Alagoas (UFAL). He is a permanent faculty member of the Graduate Program in Civil Engineering (PPGEC/CTEC/UFAL) and a researcher/coordinator at the Laboratory of Scientific Computing and Visualization (LCCV/CTEC/UFAL).

Aline da Silva Ramos Barboza: She earned a Bachelor's degree in Civil Engineering from the Federal University of Alagoas in 1987, a Master's degree in Civil Engineering (Structural Engineering) from the University of São Paulo in 1992, a Ph.D. in Civil Engineering (Structural Engineering) from the University of São Paulo in 2002, and completed postdoctoral studies at the University of São Paulo in 2016. She is a Full Professor at the Federal University of Alagoas, conducting research in structural mechanics, cast-in-place and precast concrete structures, fiber-reinforced concrete, and oil well drilling.